Particles and Fields in Radio Galaxies
ASP Conference Series, Vol. , 2001
Robert A. Laing and Katherine M. Blundell

Confronting Hydrodynamic Simulations Of Relativistic Jets With Data: What Do We Learn About Particles & Fields?

Philip A. Hughes

Astronomy Department, University of Michigan, Ann Arbor, MI 48109-1090

Abstract. We review recent relativistic hydrodynamic simulations of jets, and their interpretation in terms of the results from linear stability analysis. These studies show that, interpreted naively, the distribution of synchrotron intensity will in general be a poor guide to the physical state (density and pressure) of the underlying flow, and that even if the physical state can be inferred, it, in turn, may prove to be a poor guide to the source dynamics, in terms of the transport of energy and momentum from the central engine. However, we demonstrate that an interplay of simulation and linear stability analysis provides a powerful tool for elucidating the nature and character of structures that jets may sustain. From such studies we can explain the complex behavior of observed jets, which manifest both stationary and propagating structures, without recourse to ad hoc macroscopic disturbances. This provides a framework for the interpretation of multi-epoch total intensity data wherein an understanding of the character of individual flow features will allow the effects of physical state and dynamics to be deconvolved.

1. Introduction

While computational fluid dynamic simulations of astrophysical jets have been performed for two decades, it is only since the mid-1990s that this approach has been applied to non-steady albeit non-MHD *relativistic* flows (van Putten 1993; Duncan & Hughes 1994; Martí, Müller, & Ibáñez 1994, Martí et al., 1995, 1997; Komissarov & Falle 1998; Rosen et al. 1999). Such studies have a dual significance. Firstly, that the relativistic Euler equations are inherently more nonlinear than their classical cousins, that the Lorentz factor couples the flow along each coordinate direction, and that there is no intrinsic limit to either shock thinness or compression, imply that the distributions of density, pressure and velocity will be quite different from those computed classically. Secondly, such computations provide a physically meaningful picture of the flow dynamics, from which Doppler shift, boost, aberration and time delays may be inferred, allowing the production of simulated source maps that incorporate all the pertinent relativistic effects.

With the parallel advances in the area of VLBI/P mapping, which have led to data sets with hitherto unseen spatial, temporal and spectral resolution, and

dynamic range, it might be supposed that, by confronting these new simulations with the current and emerging data, the state and dynamics of extragalactic jets on a range of length scales could now be probed in detail. The goal of this review is to urge caution on those involved in this enterprise, a warning to the curious (James 1984) on the periphery of the subject, and encouragement that progress can be made, but that such progress is probably contingent on our acquiring a deeper understanding of jet dynamics – through, for example, carefully integrating analytic studies of jet stability with studies based on CFD simulations.

A good case can be made that, at least on observable scales, the magnetic field does not play a dynamically important role; strong evidence exists for a turbulent field in the quiescent state of both BL Lacs and QSOs (Jones et al. 1985; Hughes, Aller & Aller 1989a,b). The magnetic field responds readily to the underlying flow, and VLB polarimetry will surely provide an invaluable tool for probing jet curvature, shear and the structure of internal, in general oblique, shocks, through the imprint of these features on the field, and thus on the polarized emission. However, given the field's likely insignificance as regards the flow dynamics, and the fact that a rigorous calculation of the flow emissivity would require a knowledge of the evolution of the distribution function of the radiating particles as much as a knowledge of the magnetic field (Tregillis et al. 1999; see also Tregillis, Jones & Ryu these proceedings), for the present discussion we shall consider purely hydrodynamic flows, and the total intensity only.

2. The Intensity Distribution

Figures 1 and 2 shows simulated maps that extend the work of Mioduszewski, Hughes & Duncan (1997), for an axisymmetric flow with $\gamma_{\rm max} = 10$, $\Gamma = 4/3$, periodically ramped down to $\gamma \sim 1$. The 'mapping' assumes that the radiating particle spectrum follows $N(\epsilon)\,d\epsilon = N_0 \epsilon^{-p} d\epsilon$, $\epsilon_1 < \epsilon < \epsilon_2$, $2 < p < 3$, with N_0 determined from $n = \int N(\epsilon)\,d\epsilon$ and $e = \int N(\epsilon)\,\epsilon d\epsilon$ and assumes that $e_B \sim e$. The intensity distribution is displayed for viewing angles of 90 and 10° with and without retarded time employed. The density and pressure distributions that arise from the evolution of the inflow manifest a series of nested bow shocks, similar in form to the pattern of intensity displayed by the flow when seen in the plane of the sky. However, the intensity distribution bears little relation to the underlying pressure/density distribution, at least for rapidly evolving, partially opaque flows, when seen within tens of degrees of the flow direction. The change in source appearance with viewing angle and with the inclusion of retarded time effects, make clear the role played by Doppler boosting and source evolution respectively, and evidently these effects dominate over intrinsic emissivity in determining the (evolving) intensity distribution. The point-by-point intensity is thus a poor guide to the emissivity intergrated along a line of sight, and in the absence of a detailed knowledge of the flow dynamics, can be used neither to derive rest frame quantities such as density and pressure, nor to assess the relative values of these quantities from point to point in the source.

Indeed, the morphology of a source may exhibit unusual characteristics, suggestive of an anomalous field and/or particle distribution, or flow pattern, but

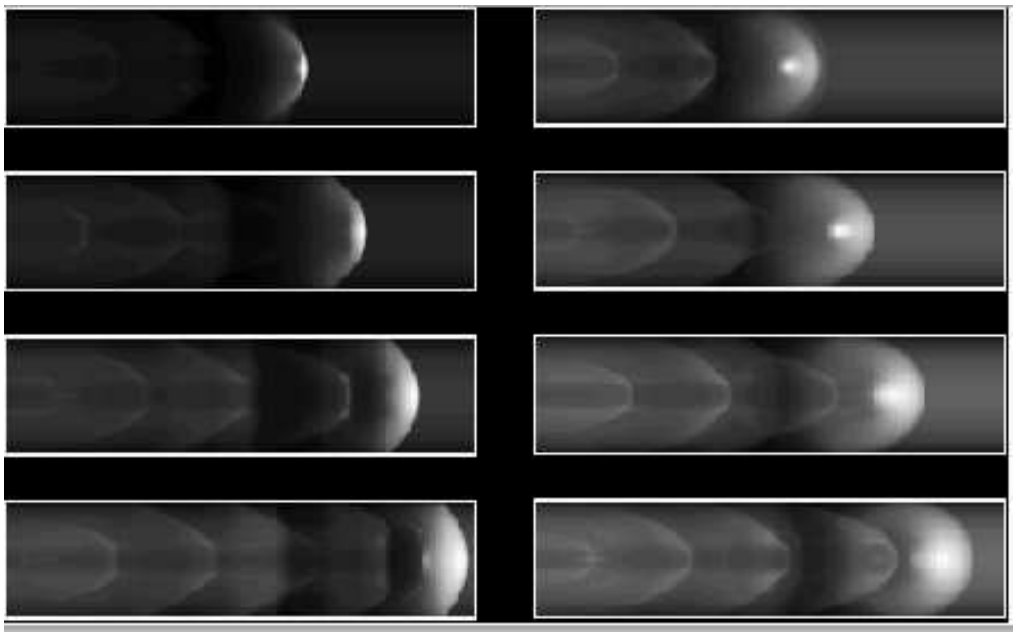

Figure 1. Simulated intensity maps for the late time evolution of a flow with $\gamma = 10$, seen at an angle 90° to the flow direction. Left: without retarded time effects; Right: with retarted time effects included.

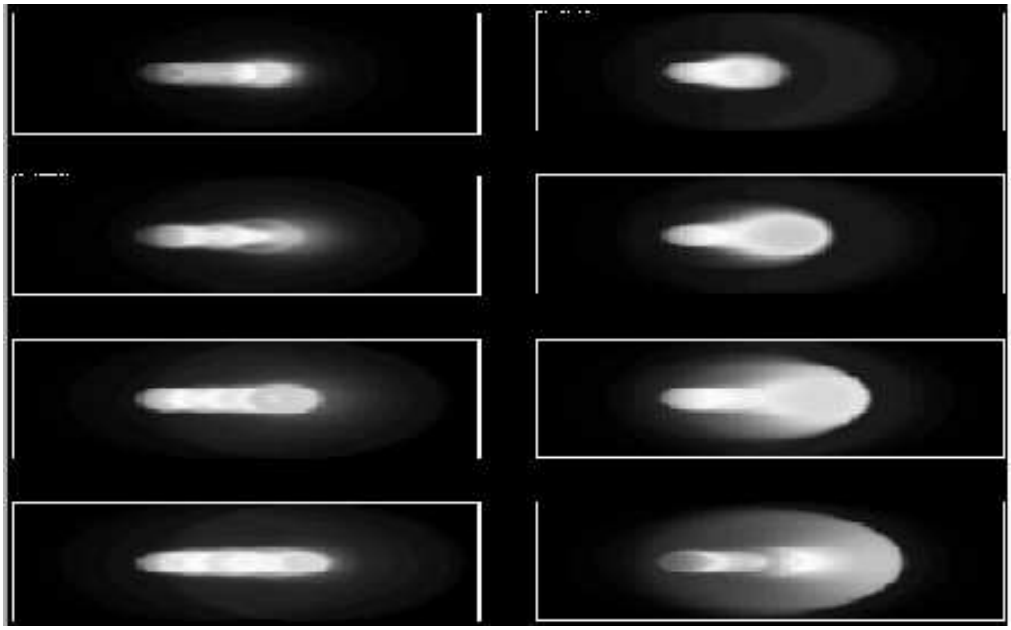

Figure 2. Simulated intensity maps for the late time evolution of a flow with $\gamma = 10$, seen at an angle 10° to the flow direction. Left: without retarded time effects; Right: with retarted time effects included.

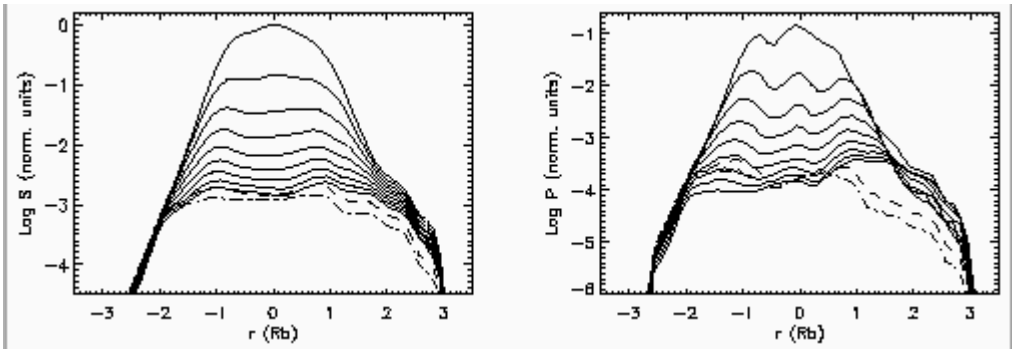

Figure 3. Left: total intensity and Right: polarized intensity profiles across a stratified jet for various viewing angles at 10° intervals between 10 and 90° (solid lines) and −130 and −170° (dashed lines). Preprinted from Aloy et al. (2000) by kind permission of the author and ApJ.

which in reality is merely a consequence of the interplay of a particular pattern of intrinsic emissivity, magnetic field geometry and Doppler boosting. Figure 3 reproduces a figure from Aloy et al. (2000) who have performed 3-D relativistic CFD jet simulations that produce a significantly stratified jet structure: a fast spine surrounded by a slower, high internal energy shear layer. The computation is purely hydrodynamic, but by assuming a distribution of magnetic field energy density and geometry related to the computed flow, the authors demonstrate that at least for a steady flow (no retarded time effects included) a significant cross-sectional asymmetry results from the ordered component of field in the sheath, which is a function of viewing angle, and which thus differs between jet and counter jet. This may well explain the curiously asymmetric structure of 1055+018 (Attridge, Roberts, & Wardle 1999), and of the BL Lac objects 0745+241, 0820+225, and 1418+546 (Pushkarev & Gabuzda, these proceedings; Gabuzda, Pushkarev & Garnich 2000). This is a valuable insight as it provides a potential method for exploring the subtleties of the magnetic field configuration in jets. However, it also drives home the point that curious and complex source morphologies do not necessarily have a parallel in either the underlying particle and field distribution or in the source dynamics – which for the example cited here constitutes a simple sheared flow and related magnetic field.

3. The Particle and Field Distribution

Let us put aside for the moment the issue of how to derive the underlying particle and field distribution from the pattern of intensity, and suppose that such information can be extracted from multi-epoch maps. To what extent can we then infer the key facets of the source dynamics – by which we mean the way energy and momentum are carried from the central engine, and the extent to which dissipation arising from naturally occurring instabilities and externally imposed perturbations influence this flux of energy and momentum?

Figure 4 shows a 3-D relativistic CFD simulation performed by the author in collaboration with M. A. Miller (Washington University) and G. C. Duncan

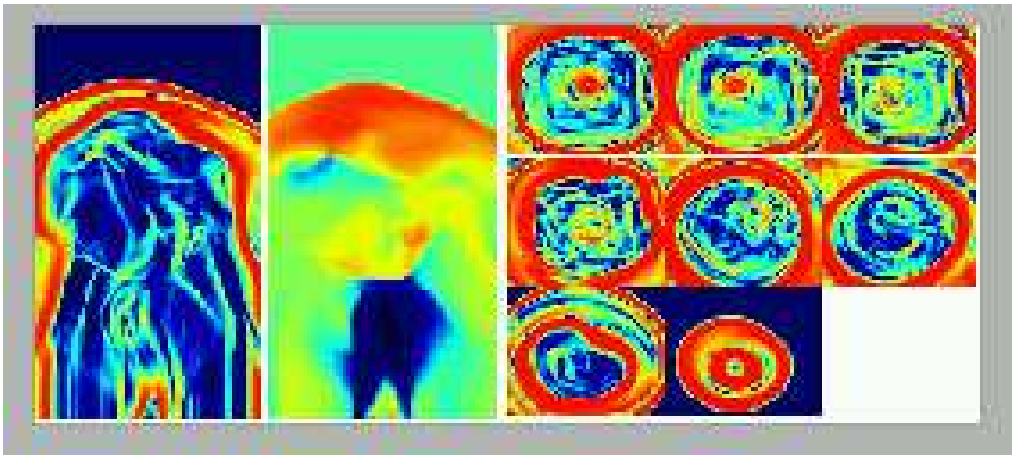

Figure 4. Left: a schlieren render of the laboratory frame density in a plane orthogonal to the inflow plane; Middle: a render of the pressure distribution on an exponential map for the same cut as shown on the left; Right: schlieren renders of the laboratory frame density for a series of cuts parallel to the inflow plane at the last computed epoch of a precessed, $\gamma = 2.5$ jet.

(Bowling Green State University) for a $\gamma = 2.5$, $\Gamma = 5/3$ jet precessing on a cone of semi-angle 11.25° with a frequency 0.2885 rad measured in time units set by the inflow radius and speed. A bubble of high pressure gas spans both the jet and the cocoon and this bubble and the network of shocks visible throughout the computational volume suggest that a complex intensity pattern would result. However, the momentum flux, $\mathcal{F} = \gamma^2 (e + p) v_z^2 + p$, persists to the bow, which is advancing at a speed $\sim 87\%$ that of the unprecessed case. Evidently, complex maps may obscure 'simple' dynamics.

Figure 5 shows the results of another simulation performed in collaboration with Miller and Duncan, in which a $\gamma = 2.5$ jet impacts an ambient density gradient inclined at 65° to the flow axis, with $n_{\rm max}/n_{\rm min} = 10$. The bow is slowed significantly by the interaction, and the 'back flow' is highly asymmetric, leading to an orthogonal **relativistic** flow with low density and pressure. As the vectors show in the rightmost panel, this backflow impacts the base of the jet, and is largely responsible for oblique internal structures set up within the jet. However, the intensity will track the Doppler boosted jet and the high pressure bow shock, not the 'relativistic deodorant spray' feature. Evidently, simple maps may obscure intriguing dynamics.

4. Understanding The Structure Of Relativistic Jets

If the intensity distribution cannot be related in a simple way to the underlying particle and field distributions, and given that (even if some approach enabled these distributions to be elucidated) they may give a very misleading impression concerning the essential flow dynamics, is it possible to make any progress in the interpretation of total intensity maps; in particular, by confronting the results

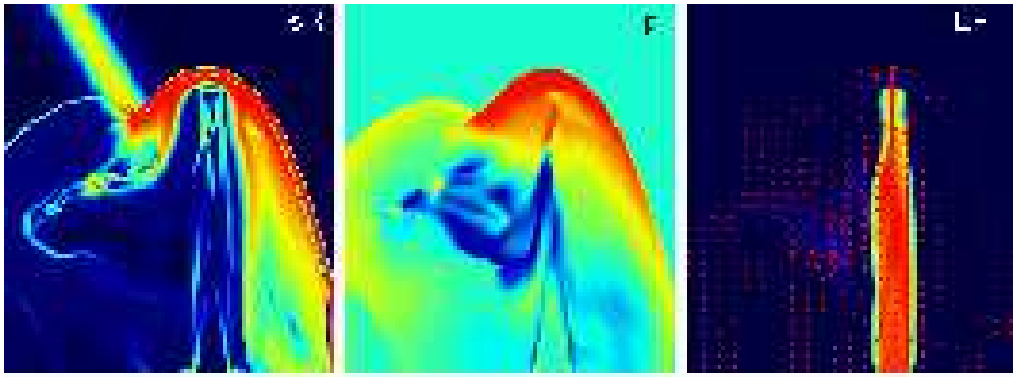

Figure 5. Left: a schlieren render of the laboratory frame density in a plane orthogonal to the inflow plane; Middle: a render of the pressure distribution on an exponential map for the same cut as shown on the left; Right: a map of the Lorentz factor, with velocity 3-vectors superposed, at the last computed epoch for a $\gamma = 2.5$ jet interacting with an ambient density gradient.

of CFD simulations with such data? The problems have arisen because of our attempt to relate synchrotron intensity to physical state, and physical state to dynamics. However, the total intensity map contains too little information to allow this to be done uniquely. Further constraints are needed, and we suggest that a promising way forward is to interpret the data in the context of an understanding of what structures jets could and do support. Specifically, as we shall now show, by combining the results of CFD simulations with the results of first order stability analysis, we can both understand the nature and origin of features evident in the simulations, and demonstrate that, contrary to expectation, we may use a linear stability analysis to predict the large amplitude flow features evident in data and simulations. While simulation provides a vital check on the predictions of linear stability analysis, and is essential for reproducing the detailed flow pattern, the stability analysis provides a tool for rapidly exploring a wide range of parameter space, and simple, idealized models of flow structures. Future application of these studies as a tool to aid in the interpretation of data impose two requirements. Firstly, that our ability to recognize and understand flow features as (possibly Doppler boosted and aberrated) distinct modes of the Kelvin-Helmholtz instability (which may have steepened to form shocks) be tested in the simplest possible case – slowly evolving, transparent kiloparsec-scale flows. Secondly, that the signature of such structures in rapidly evolving, partially opaque flows be computed for comparison with data on the more challenging parsec-scale flows.

5. The Structure of Axisymmetric Jets

Figures 6 and 7 shows simulations of axisymmetric jets with $\gamma = 2.5$, $\Gamma = 5/3$ and $\gamma = 10.0$, $\Gamma = 4/3$ respectively, performed by the author in collaboration with Duncan. In collaboration with P. E. Hardee and A. Rosen (University of

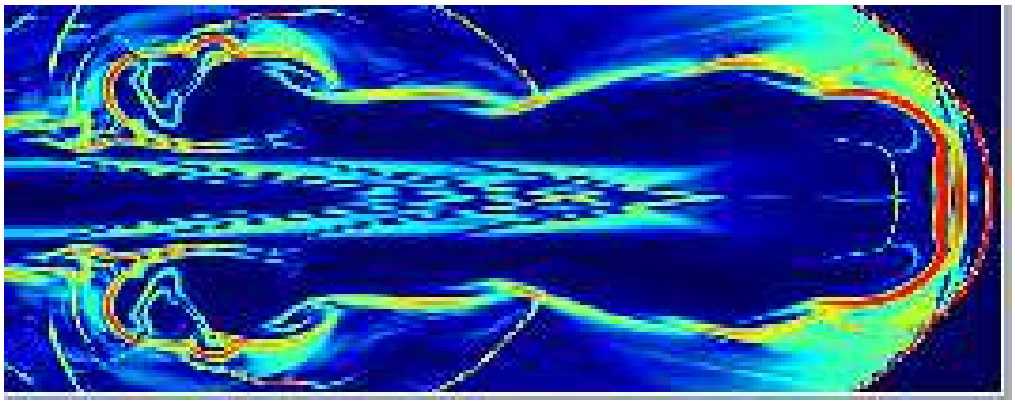

Figure 6. A schlieren render of the laboratory frame density for an axially symmetric jet with inflow Lorentz factor $\gamma = 2.5$.

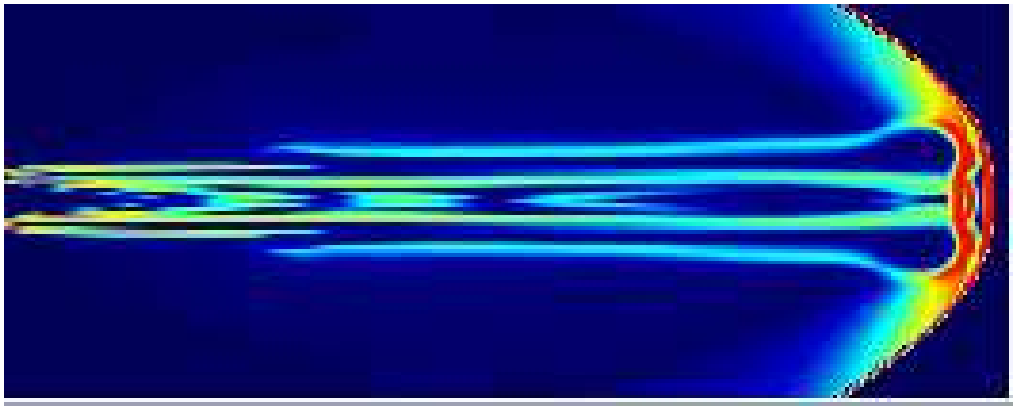

Figure 7. A schlieren render of the laboratory frame density for an axially symmetric jet with inflow Lorentz factor $\gamma = 10.0$.

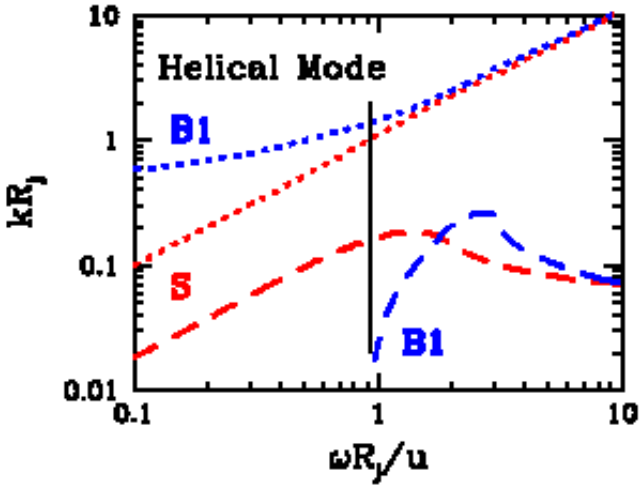

Figure 8. The dispersion relation used to motivate the 3-D jet perturbations. cf. Hardee 2000.

Alabama) a first order Kelvin-Helmholtz stability analysis (Hardee et al. 1998) has been used to identify the internal jet structure seen in Figure 6 as due to driving of the third body mode (B_3) by pressure perturbations associated with the cocoon vortices that arise due to instability of the contact surface between shocked jet and shocked ambient material. In contrast, the slight internal jet structure seen in Figure 7 has been associated with driving of the first body mode (B_1) by the conical pressure wave at the inlet; furthermore, the wavelength and obliquity of the perturbation do not well match those of the excited mode, and this weak coupling explains why the mode is barely evident.

6. The Structure of 3-D Jets

Our success in understanding the structure of axisymmetric flows in 2-D has prompted us to apply the same principles to 3-D jets (see Figure 8), where instability is likely to play a more important role, as the higher order modes – suppressed in axisymmetry – can manifest themselves. Figure 9 shows a simulation performed by the author in which a pre-existing jet with $\gamma = 2.5$, $\Gamma = 5/3$ has been subject to a low amplitude precessional perturbation ($v_\perp < 1\% v_{\rm jet}$) at the inflow. This configuration was adopted so as to avoid having to devote valuable computational resources to facets of the dynamics – the contact surface and bow shock – not directly related to the issue of internal jet structure, and to provide an environment in which the jet could be excited with carefully selected perturbations. This scenario corresponds to an epoch long after the jet head and bow shock have passed by, and the jet is cocooned by a *light* medium – the shocked jet material. We have adopted a density ratio of $n_{\rm jet}/n_{\rm amb} = 10.0$. Three perturbation frequencies have been explored: low (L), with $\omega R_{\rm jet}/v_{\rm jet} = 0.40$; intermediate (I) with $\omega R_{\rm jet}/v_{\rm jet} = 0.93$; and high (H), with $\omega R_{\rm jet}/v_{\rm jet} = 2.69$. The values were chosen to excite either or both the helical surface and first body modes, using dispersion relations computed by Hardee – see Figure 8.

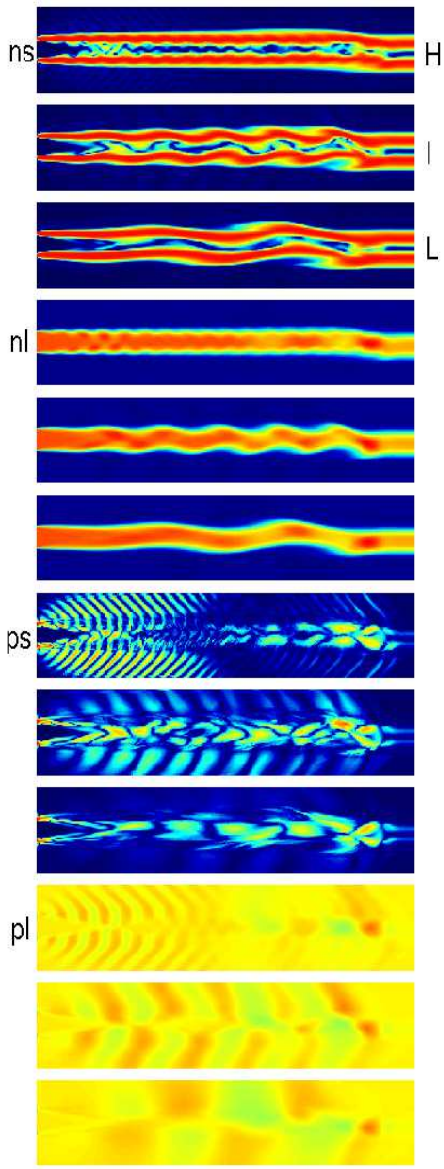

Figure 9. Renders of rest frame density (n) and pressure (p) in schlieren (s) and linear (l) maps, for the high, intermediate and low (H, I, L) frequency perturbations of a preexisting $\gamma = 2.5$, $\Gamma = 5/3$ jet.

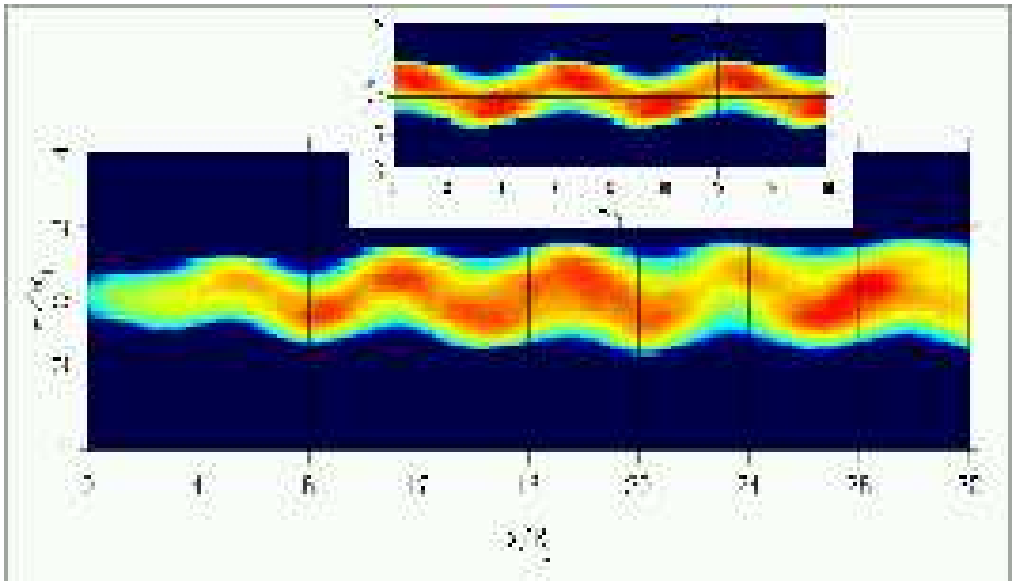

Figure 10. Main: the line of sight integral of p^2 for the intermediate frequency perturbation shown in Figure 9; Inset: the same diagnostic, computed for a jet reconstructed from a first order stability analysis, assuming that the jet structure is dominated by the helical surface mode.

An important, but sometimes overlooked, aspect of the stability analysis is that we can go beyond simply computing dispersion relations, and for one or a set of modes 'reconstruct' the flow pattern that arises as a consequence of their development. Specifically, we can relate all components of the fluid displacements at some r to radial displacement at $R_{\rm jet}$, the variations in state variables such as p at any r to the displacements in fluid at that r, and the velocity components of perturbations at some r to the time derivative of displacements in the fluid at that r. Thus for some adopted surface pressure fluctuation, surface displacement, or whatever, we can construct a detailed picture of a perturbed jet. An apparent (and possibly severe) limitation of this reconstruction is the very nature of the stability analysis: it assumes infinitesimal perturbations. One might thus suspect that it would be incapable of predicting the large amplitude structures that will result in CFD simulations.

To explore this issue, let us focus on case 'I' described above. Figure 10 shows a comparison of the simulated flow with a reconstruction that assumes the helical surface mode dominates, using the line of sight integral of p^2 as a diagnostic. Remarkably, we see that the numerical simulation has excited a well-defined mode of the Kelvin-Helmholtz instability, and that the first order analysis has done an excellent job of predicting jet structure. A full analysis of the simulations shown in Figure 9 in the context of the normal modes analysis shows that due to excitation of the surface and first body modes, the jet exhibits propagating structures with speeds between $0.62c$ and $0.86c$, that fastest moving structures traveling at a speed not much less than that of the underlying fluid

flow; but furthermore, due to a beating between these modes, a pattern of stationary structures also occurs. Thus the complex behavior of real jets (e.g, that of M 87) may be both reproduced and understood in terms of structures that inevitably develop in response to small perturbations, and need not be supposed to arise from some unspecified physics hidden in the unresolved inner regions of the source.

7. Conclusions

Significantly perturbed jets continue to carry energy and momentum far from their origin, but a) the intensity maps may be a poor guide to the energy and density distributions; b) the energy and density distributions may be a poor guide to the source dynamics. We suggest that the interpretation of total intensity data will be facilitated if it can be done in the context of understanding the internal structures that jets may and do support. Specifically, linear stability analysis aids in the interpretation of CFD simulations, while the latter validate extrapolating stability analysis into the nonlinear regime to predict jet structures. We thus have a powerful set of tools with which to confront the most easily addressed data sets – those involving slow moving, optically thin features (e.g., as seen in M 87). The CFD simulations suggest that jets subject to particular disturbances may exhibit a few, identifiable modes, and if we can test our theoretical tools on data such as that available for M 87, we will be in a position to predict the characteristics of the modes most likely to influence jet structure, for the more challenging case of rapidly evolving, partially absorbed flows.

Acknowledgments. This work was supported by NSF grant AST 9617032 and by the Ohio Supercomputer Center.

References

Aloy, M.-A., Gómez, J.-L., Ibáñez, J. M.ª Martí, J. M.ª, & Müller, E. 2000, 'Radio Emission from Three-dimensional Relativistic Hydrodynamic Jets: Observational Evidence of Jet Stratification' ApJ, 528, L85–L88

Attridge, J. M., Roberts, D. H., & Wardle, J. F. C. 1999, 'Radio Jet-Ambient Medium Interactions on Parsec Scales in the Blazar 1055+018', ApJ, 518, L87–L90

Duncan, G. C., & Hughes, P. A. 1994, 'Simulations of Relativistic Extragalactic Jets', ApJ, 436, L119–L122

Gabuzda, D. C., Pushkarev, A. B., & Garnich, N. N. 2000, 'Unusual Radio Properties of the BL Lac Object 0820+225', MNRAS, submitted

Hardee, P. E. 2000, 'On the 3D Structure of Relativistic Hydrodynamic Jets', ApJ, 533, 176–193

Hardee, P. E., Rosen, A., Hughes, P. A., & Duncan, G. C. 1998, 'Time Dependent Structure of Perturbed Relativistic Jets', ApJ, 500, 599–609

Hughes, P. A., Aller, H. D., & Aller, M. F. 1989a, 'Synchrotron Emission from Shocked Relativistic Jets. I. The Theory of Radio-Wavelength Variability and its Relation to Superluminal Motion', ApJ, 341, 54–67

Hughes, P. A., Aller, H. D., & Aller, M. F. 1989b, 'Synchrotron Emission from Shocked Relativistic Jets. II. A Model for the Centimeter Waveband Quiescent and Burst Emission from BL Lacertae', ApJ, 341, 68–79

James, M. R. 1984, 'A Warning To The Curious', in The Penguin Complete Ghost Stories of M. R. James (New York: Penguin Books), 314–327

Jones, T. W., Rudnick, L., Aller, H. D., Aller, M. F., Hodge, P. E., & Fiedler, R. L. 1985, 'Magnetic Field Structures in Active Compact Radio Sources', ApJ, 290, 627–636

Komissarov, S. S., & Falle, S. A. E. G. 1998, 'The Large-Scale Structure of FR-II Radio Sources', MNRAS, 297, 1087–1108

Martí, J. M.$^{\underline{a}}$, Müller, E., Font, J. A., & Ibáñez, J. M.$^{\underline{a}}$ 1995, 'Morphology and Dynamics of Highly Supersonic Relativistic Jets', ApJ, 448, L105–L108

Martí, J. M.$^{\underline{a}}$, Müller, E., Font, J. A., Ibáñez, J. M. Z., & Marquina, A. 1997, 'Morphology and Dynamics of Relativistic Jets', ApJ, 479, 151–163

Martí, J. M.$^{\underline{a}}$, Müller, E., & Ibáñez, J. M.$^{\underline{a}}$ 1994, 'Hydrodynamical Simulations of Relativistic Jets', A&A, 281, L9–L12

Mioduszewski, A. J., Hughes, P. A., & Duncan, G. C. 1997, 'Simulated VLBI Images from Relativistic Hydrodynamic Jet Models', ApJ, 476, 649–665

van Putten, M. H. P. M. 1993, 'A Two-Dimensional Relativistic (Gamma = 3.25) Jet Simulation', ApJ, 408, L21–L23

Rosen, A., Hughes, P. A., Duncan, G. C., & Hardee, P. E. 1999, 'A Comparison of Relativistic and Nonrelativistic Jet Simulations', ApJ, 516, 729–743

Tregillis, I. L., Jones, T. W., Ryu, D., & Park, C. 1999, 'Simulations of Nonthermal Electron Transport in Multidimensional Flows: Synthetic Observations of Radio Galaxies', astro-ph/9908316